Neurochemical Research (2020) 45:2939–2948
https://doi.org/10.1007/s11064-020-03142-8

ORIGINAL PAPER

Cephalic Neuronal Vesicle Formation is Developmentally Dependent and Modified by Methylmercury and *sti-1* in *Caenorhabditis elegans*

Tao Ke[1] · Abel Santamaria[2] · Joao B. T. Rocha[3] · Alex Tinkov[4,5] · Julia Bornhorst[6] · Aaron B. Bowman[7] · Michael Aschner[1,5,8]

Received: 20 July 2020 / Revised: 26 September 2020 / Accepted: 1 October 2020 / Published online: 10 October 2020

Abstract

Methylmercury (MeHg) is a potent neurotoxicant. The mechanisms underlying MeHg-induced neurotoxicity are not fully understood. Several studies have shown that protein chaperones are involved in MeHg toxicity. The protein co-chaperone, stress inducible protein 1 (STI-1), has important functions in protein quality control of the chaperone pathway. In the current study, dopaminergic (DAergic) cephalic (CEP) neuronal morphology was evaluated in the *Caenorhabditis elegans* (*C. elegans*) *sti-1* knockout strain. In the control OH7193 strain (dat-1::mCherry + ttx-3::mCherry), we characterized the morphology of CEP neurons by checking the presence of attached vesicles and unattached vesicles to the CEP dendrites. We showed that the attached vesicles were only present in adult stage worms; whereas they were absent in the younger L3 stage worms. In the *sti-1* knockout strain, MeHg treatment significantly altered the structures of CEP dendrites with discontinuation of mCherry fluorescence and shrinkage of CEP soma, as compared to the control. 12 h post treatment on MeHg-free OP50-seeded plates, the discontinuation of mCherry fluorescence of CEP dendrites in worms treated with 0.05 or 0.5 μM MeHg returned to levels statistically indistinguishable from control, while in worms treated with 5 μM MeHg a higher percentage of discontinuation of mCherry fluorescence persisted. Despite this strong effect by 5 μM MeHg, CEP attached vesicles were increased upon 0.05 or 0.5 μM MeHg treatment, yet unaffected by 5 μM MeHg. The CEP attached vesicles of *sti-1* knockout strain were significantly increased shortly after MeHg treatment, but were unaffected 48 h post treatment. In addition, there was a significant interactive effect of MeHg and *sti-1* on the number of attached vesicles. Knock down *sti-1* via RNAi did not alter the number of CEP attached vesicles. Taking together, our data suggests that the increased occurrence of attached vesicles in adult stage worms could initiate a substantial loss of membrane components of CEP dendrites following release of vesicles, leading to the discontinuation of mCherry fluorescence, and the formation of CEP attached vesicles could be regulated by *sti-1* to remove cellular debris for detoxification.

Keywords Methylmercury · CEP neuron · Stress inducible protein 1 · Microvesicle

✉ Michael Aschner
michael.aschner@einstein.yu.edu

[1] Department of Molecular Pharmacology, Albert Einstein College of Medicine, Bronx, NY 10461, USA

[2] Laboratorio de Aminoácidos Excitadores, Instituto Nacional de Neurología y Neurocirugía, Mexico City 14269, Mexico

[3] Department of Biochemistry and Molecular Biology, Federal University of Santa Maria, Santa Maria, RS, Brazil

[4] Yaroslavl State University, Sovetskaya St., 14, Yaroslavl, Russia 150000

[5] IM Sechenov First Moscow State Medical University, Sechenov University, Moscow, Russia

[6] Food Chemistry, Faculty of Mathematics and Natural Sciences, University of Wuppertal, Wuppertal, Germany

[7] School of Health Sciences, Purdue University, West Lafayette, IN 47907-2051, USA

[8] Department of Molecular Pharmacology, Albert Einstein College of Medicine, 1300 Morris Park Avenue Forchheimer Building, Room 209, Bronx, NY 10461, USA

Introduction

A decline in cellular homeostasis control and concomitant structural and functional decay is fundamental for the development of age-related diseases [1]. Distinct from cells with a self-renewal potential, post-mitotic neurons are vulnerable for the decline of protein quality control, a system for surveillance and maintaining the proper structure and function of proteins by facilitating folding of nascent/misfolded proteins and degradation of protein aggregates [2]. Protein quality control encompasses several systems geared towards a coordinated and efficient work stream, and it includes molecular-chaperone assisted protein refolding, proteasomal degradation of soluble misfolded proteins and degradation of insoluble protein aggregates by lysosomes [3]. Nearly 10% of the proteome in a eukaryotic cell are molecular chaperones, which play important roles in basal as well as regulated responses of protein quality control to cellular stress, such as oxidative stress, toxic chemicals, inflammation, and heat shock [2]. Molecular chaperones facilitate refolding and unfolding of nascent and misfolded proteins, and they also play a role in degradation of misfolded proteins by delivering them to proteasome, and lysosome which also refers to chaperone-mediated autophagy (CMA) [4].

The majority of molecular chaperones are heat shock proteins which were named after their increased synthesis in response to heat shock [2]. Heat shock proteins have essential roles in the process of protein synthesis, folding, and transport [1]. Methylmercury (MeHg) is an environmental neurotoxicant that bioaccumulates in the marine food chain. Human exposure to environmental MeHg mainly occurs through the consumption of fish, which poses a significant health threat to developing children [5]. In a previous study, we showed that short time exposure (1–6 h) of astrocytes to the neurotoxicant MeHg, the binding activity of the heat shock protein 90 (Hsp90) with its client proteins (prostaglandin E synthase and nitric oxide synthase) was significantly increased, while a prolonged exposure (12–24 h, 1 μM MeHg) eventually repressed the expression of Hsp90, leading to aberrant regulation of redox homeostasis, a hallmark of MeHg's neurotoxicity [6]. It is empirical that proteins rich in sulfhydryl (-SH) groups with structural and functional importance are potential targets of MeHg [7–9]. This has been confirmed with studies on heat shock factor 1 (HSF1), an evolutionarily conserved transcription factor that initiates transcription of heat shock proteins including Hsp90 and heat shock protein 70 (Hsp70) [10, 11]. Embryonic exposure to MeHg (5 ppm) has been shown in mice cortices to induce nuclear translocation of HSF1, and a more than 4-fold increase in the association of HSF1 with the *Hsp70* promoter [12]. In contrast to wild-type mice, in *Hsf1* knockouts, MeHg treatment caused a significant decline in brain weight at postnatal day 25 (P25), reduced rate of neurogenesis, and increased rate of neuronal apoptosis and seizure susceptibility [12]. Furthermore, siRNA mediated silencing of *Hsf1* in HEK 293 cells caused an elevation of cell death rate in response to MeHg [13].

The Hsp70 and Hsp90 organizing protein (Hop), or stress inducible protein 1 (STI-1) transfers client proteins from Hsp70 to Hsp90 [14, 15]. Intracellular STI-1 is a co-chaperone that assists protein folding in the intermediate stage of the Hsp70/Hsp90 pathway by transferring client proteins from the early complex (Hsp70/Hsp40) to the intermediate complex (Hsp70/Hsp90) [16]. Genetic studies in yeast cells have revealed that deletion of *sti-1* reduces the *in vivo* activity of the Hsp90 client protein, glucocorticoid receptor (GR) [14]. STI-1 is a conserved protein across phyla, and the biological activities in some species were delineated. *Sti-1* knockout mice are embryonic lethal [17], while *sti-1* knockout *Caenorhabditis elegans* (*C. elegans*) is viable [18].

Previously, we have shown that the morphology of *C. elegans* dopaminergic (DAergic) cephalic (CEP) dendrites is a target of MeHg [19], featuring focal aggregation of mCherry molecules in CEP dendrites. We showed that MeHg could induce bright puncta of *dat-1*::mCherry aggregates in the dendrites of CEP dopaminergic neurons in a dose- and time-dependent manner. We compared the size and brightness of the puncta with the intracellular mCherry inclusions in neuronal soma, and concluded that the enlarged sphere shape of bright mCherry puncta at the CEP dendrites was the hallmark of the toxic effects of chronic MeHg exposure [19]. Recently, in a study with *Drosophila* Huntington's disease (HD) model, it shows that the STI-1 homolog, Hop, is involved in the aggregation of mutant Huntingtin (*mHtt*) [20]. In the *C. elegans* OH7193 strain, the typical morphology of CEP neuron is the presence of extracellular mCherry and "dot" like vesicular structures in the dendrites [21, 22]. The extracellular mCherry of CEP neuron can be released through the formation of vesicular structures [22]. In the *sti-1* knockout strain (VC2559), we observed that they were reproductively healthy, but the DAergic CEP morphology was significantly altered, with a significant loss of the mCherry fluorescence in CEP dendrites after MeHg exposure. In the current study, we report the findings of CEP morphology in the *sti-1* knockout strain in response to MeHg.

Materials and Methods

C. elegans Strains and Maintenance

Caenorhabditis elegans strains were maintained on NGM plates at 20 °C. The OH7193 [otIs181 III; him-8(e1489)

IV], VC2559 [sti-1(ok3354) V], and TU3311 [unc-119p::YFP + unc-119p::sid-1] strains were obtained from the Caenorhabditis Genetic Center (University of Minnesota). To cross the OH7193 strain with the VC2559 strain, 6–10 young adult stage OH7193 male worms were mated with 4–6 late L4 stage hermaphrodites of VC2559. After 7–8 days, the F2 homozygotes of mCherry were genotyped for *sti-1* with single worm PCR (duplex PCR, forward primer 1: 5′GCTCAGCGAGCCTACGAAGATG3′, forward primer 2: 5′CCAGAGAGCTCTTGATGATTGTGAC3′, reverse primer: 5′TGAAGACGAGTCCAGAGGACG3′). Synchronization of worm cultures was achieved by bleaching of gravid hermaphrodites and sucrose separation to harvest eggs. The harvested eggs were incubated at 20 °C for 18 h.

MeHg Exposure

MeHg (Sigma-Aldrich) was dissolved in ddH_2O to make 40 × stock solution (2, 20, 200 µM MeHg). Synchronized Larvae stage 1 (L1) worms were treated in NGM medium (3 g NaCl, 2.5 g peptone, 975 ml H_2O, 1 ml cholesterol (5 mg/ml in ethanol), 1 ml nystatin, 1 ml 1 M $CaCl_2$, 1 ml 1 M $MgSO_4$, 25 ml 1 M pH 6 KPO_4), at 160 rpm with dead OP50 bacteria. We showed that ~ 34% of worms died upon chronic MeHg exposure when fed with live bacteria; however, the dead OP50 fed- worms were alive at the end of exposure [19]. Dead bacteria were prepared by heating 1 ml concentrated (100×) overnight cultured OP50 in 80 °C incubator for 1 h [23]. After treatment, worms were transferred to OP50 seeded NGM plates for further analysis. The concentrations of MeHg used for the experiment are 0, 0.05, 0.5, and 5 µM.

Imaging of Vesicular Structures

Attached vesicles and unattached vesicles are pre-defined neuronal structures as shown in Fig. 1. Following MeHg treatment, worms were paralyzed with 3 mM levamisole (Sigma, catalog number: 1359302). They were imaged with confocal microscope (Leica SP8, Germany). The images of CEP dendrites were obtained via 40 × object (Leica SP8, Germany). Parameters including wavelength and energy

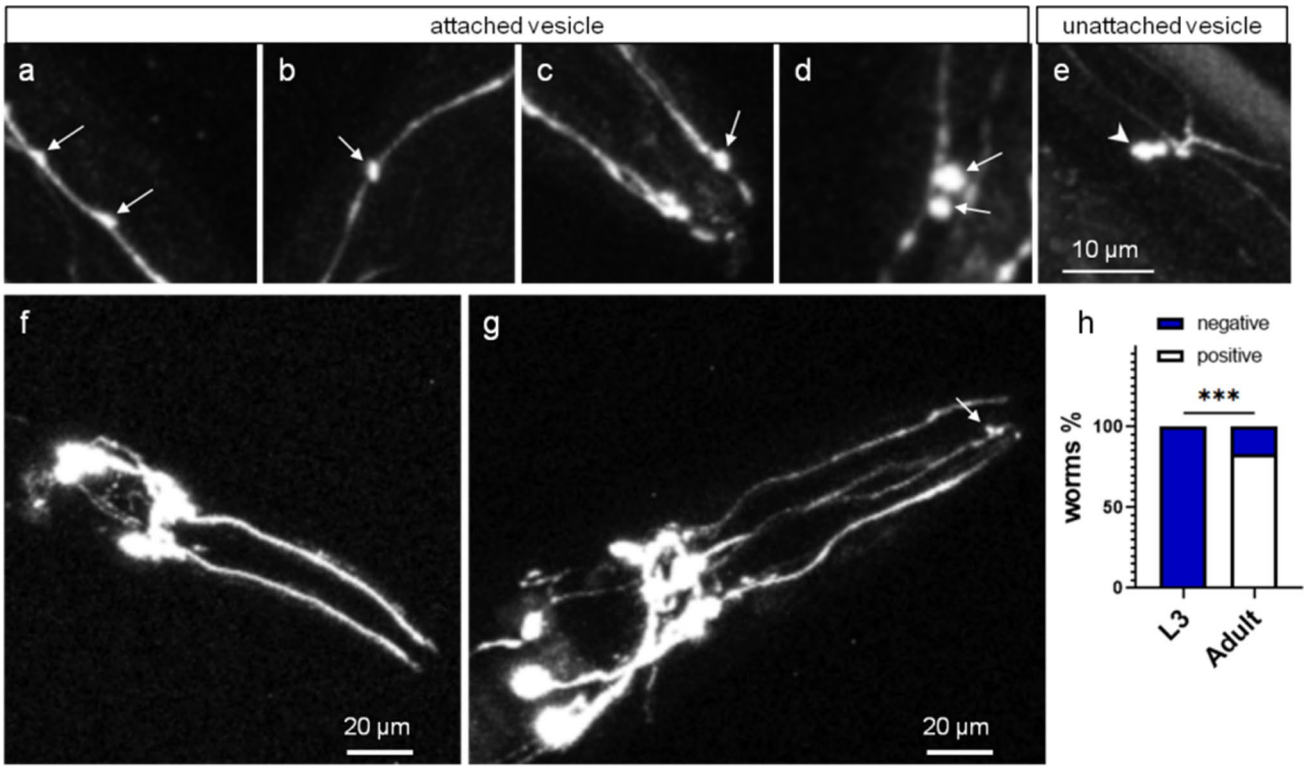

Fig. 1 Attached vesicles are associated with developmental stage. The OH7193 strain was imaged with Leica SP8 confocal microscope. **a**–**d** Shows different stages of attached vesicles (**a** and **b**: early stage; **c**: mediate stage; **d**: late stage) budding from CEP dendrites. The presence of an attached vesicle is judged by the angle (≥ 30 degree) of membrane curvature in CEP dendrite. **e** A mature unattached vesicle is released from CEP dendrite. **f** Shows the head region of a L3 stage worm. The anterior side is on the right. **g** Shows the head region of an adult stage worm. The anterior side is on the right. The arrow in **g** shows an attached vesicle is budding from the ending of CEP dendrite. **h** Percentage of worms (L3 and adult stage) with positive attached vesicles in CEP dendrites. 25–30 worms for each group were analyzed. Comparison was made with Chi-square test. ***$P < 0.001$

of excitation light, magnification factor, emission gating range, and scanning speed were analogous during image acquisition.

Counting of Vesicles

To evaluate the number of CEP attached vesicles and unattached vesicles, worms were placed on a 2% agarose pad, and paralyzed with 3 mM levamisole. They were evaluated with epifluorescence microscope (Olympus BX41). The investigator was blinded to genotype. The complete 3D-structure of CEP neurons can be observed by slightly turning forward and backward of the fine adjustment knob of the microscope. 15–30 worms per group were evaluated.

Feeding RNAi

The TU3311 strain was crossed with the OH7193 strain to generate a strain for CEP morphological evaluation following RNAi. To knock down *sti-1* by feeding RNAi, L1 stage worms were fed with the bacteria clone with RNAi plasmid targeting the sequence of R09E12.3 (*sti-1*). After 7 days, the F1 adult stage worms of TU3311*OH7193 strain were treated with MeHg in NGM medium of RNAi bacteria with isopropylthio-β-galactoside (IPTG, 1 mM) and carbenicillin (100 μg/ml).

Statistical Analysis

All data were computed and analyzed with the software GraphPad 8.0.2 (La Jolla, CA, USA). To analyze data that conforms to a normal distribution (Shapiro-Wilk test), t-test, or one-way ANOVA and post hoc Tukey's multiple comparisons test were performed. For data that conforms to a Chi-square distribution, they are analyzed with Chi-square test followed by Chi-square partition method for multiple comparisons. To analyze the effects of RNAi and MeHg, the data were compared with two-way ANOVA test. For all analysis, $p \leq 0.05$ was considered to be statistically significant.

Result

In characterizing the morphology of *C. elegans* CEP neurons, we observed a significant transition in the morphology of CEP neurons during development. In adult stage worms of the OH7193 strain, vesicular structures can be formed in the CEP dendrites. Some of these vesicular structures were attached to CEP dendrites (attached vesicles), and others had a clear boundary with CEP dendrites (unattached vesicles) (Fig. 1). We found that the attached vesicles were only present in adult stage worms compared with L3 stage worms (Fig. 1). More than 80% of adult stage worms were positive for the presence of attached vesicles in the CEP dendrites, whereas no worms in the younger L3 stage had the structure (Fig. 1).

In the OH7193 strain, the integrity of CEP structures revealed by mCherry fluorescence was not significantly affected by MeHg (Fig. 2a). However, in the *sti-1* knockout strain (VC2559*OH7193, Fig. 2b, c), MeHg treatment significantly altered the structures of CEP with discontinuation of mCherry fluorescence in CEP dendrites and shrinkage of CEP soma (Fig. 2b). In some cases, the mCherry fluorescence from CEP neurons were completely lost (Fig. 2c). In the *sti-1* knockout strain, treatment with 0.05 μM MeHg significantly increased the percentage of worm with the positive phenotypes as shown in Fig. 2b, c. 0.5 μM MeHg had a tendency to increase the percentage of worm with the positive phenotypes ($p = 0.09$). However, there was no significant difference in the percentages between worms with 5 μM MeHg and control worms (Fig. 2d). 12 h post treatment on MeHg-free OP50-seeded plates, the integrity of mCherry fluorescence in the *sti-1* knockout worms treated with 0.05 or 0.5 μM MeHg recovered to levels statistically indistinguishable from controls, suggesting it is a reversible process. It is noteworthy that the *sti-1* knockout worms treated with 5 μM MeHg had a significantly higher percentage of the phenotypes compared with the OH7193 control 12 h post treatment (Fig. 2e).

The compromised integrity of CEP neuron in the *sti-1* knockout strain compared to the OH7193 control led us to next evaluate the vesicular structures in CEP dendrites. In the *sti-1* knockout strain, we noted that the number of attached vesicle was significantly increased upon 0.05 μM MeHg treatment (Fig. 3b). The number of attached vesicles in worms treated with 0.5 μM MeHg was higher than that in control worms, but the difference did not attain statistical significance ($p = 0.056$). The number of attached vesicles in worms treated with 0.05 or 0.5 μM MeHg was significantly higher than in worms treated with 5 μM MeHg (Fig. 3b). Meanwhile, the number of attached vesicles in worms treated with 5 μM MeHg was statistically indistinguishable from controls (Fig. 3b). Moreover, we noted that the percentage of worms with positive unattached vesicles was also significantly increased upon treatment with 0.05 μM MeHg (Fig. 3c). The percentage of unattached vesicles in worms treated with 0.05 or 0.5 μM MeHg was significantly higher than that in worms treated with 5 μM MeHg. The 5 μM MeHg treatment had no significant effect on the percentage of worms with unattached vesicles (Fig. 3c).

In order to investigate if the CEP morphology persists after MeHg treatment, the *sti-1* knockout strain was treated with graded concentrations of MeHg, and evaluated at adult stage 48 h post treatment (Fig. 4). We found that at adult

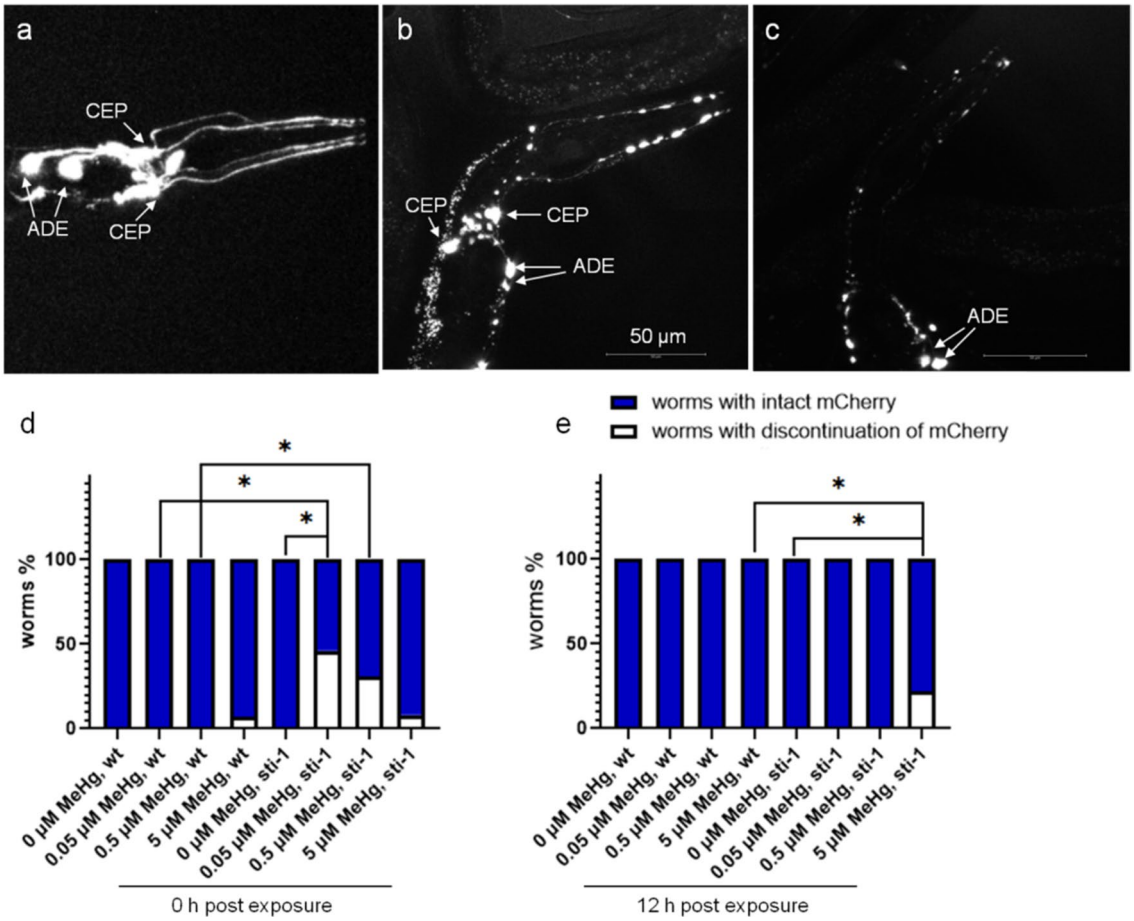

Fig. 2 Discontinuation of CEP dendritic mCherry is induced by MeHg in *sti-1* knockout strain. The OH7193 and VC2559*OH7193 strains were imaged at adult stage following MeHg treatment (0, 0.05, 0.5, and 5 µM) in NGM medium for 7 days. **a** Shows an adult stage OH7193 worm with intact and continual mCherry signals from CEP dendrites. **b** Shows an adult stage worms of VC2559*OH7193 strain with discontinuation of mCherry signals from CEP dendrites and shrinkage of CEP soma. **c** Shows an adult stage worms VC2559*OH7193 strain with disappearance of mCherry signals from CEP dendrites and CEP soma, while those from ADE are relatively intact. Worms having a similar phenotype shown in (**b**) or (**c**) are classified as discontinuation of mCherry. **d** percentage of worms with the discontinuation of mCherry following MeHg treatment. **e** Percentage of worms with the discontinuation of mCherry 12 h post MeHg treatment. Analysis was made with Chi-square test. *$P < 0.05$

stage 48 h post treatment, the differences amongst the groups were indistinguishable (Fig. 4).

To determine if the effects of MeHg are dependent of *sti-1*, the OH7193 control and *sti-1* knockout strain (VC2559*OH7193) were treated with 5 µM MeHg. Forty eight hours post-treatment, the number of attached vesicles was not changed with MeHg, but the VC2559*OH7193 strain had a significantly higher number of attached vesicles compared with the OH7193 control (Fig. 5a). Two-way ANOVA analysis indicated a significant main effect of *sti-1* knockout on the number of attached vesicles ($F(1,71) = 38.65$; $P < 0.001$). Moreover, the interaction *sit-1* knockout with MeHg treatment was also significant ($F(1,71) = 3.93$, $P = 0.05$). MeHg treatment decreased the number of attached vesicles in the OH7193 control (wt), but not in the *sti-1* knockout strain (sti-1) (Fig. 5b).

The results obtained in the adult stage *sti-1* knockout worms (Figs. 4 and 5) suggest that the attached vesicles are induced when worms are actively treated with MeHg. Accordingly, next we evaluated adult stage *sti-1* knockout strain worms upon treatment with graded concentrations of MeHg for 24 h. In this experiment, the morphology of CEP neurons was evaluated immediately after treatment. After a 24-h treatment in NGM medium, the number of attached vesicles in *sti-1* knockout strain was significantly increased upon 0.05–0.5 µM MeHg treatment (Fig. 6a). However, the number of attached vesicles in the group with 5 µM MeHg was not significantly different from the control. In addition, differences in the number of unattached vesicles did not attain statistical significance (Fig. 6b).

The TU3311 strain is hypersensitive to neuronal RNAi. To knockdown *sti-1*, the TU3311 strain was crossed with

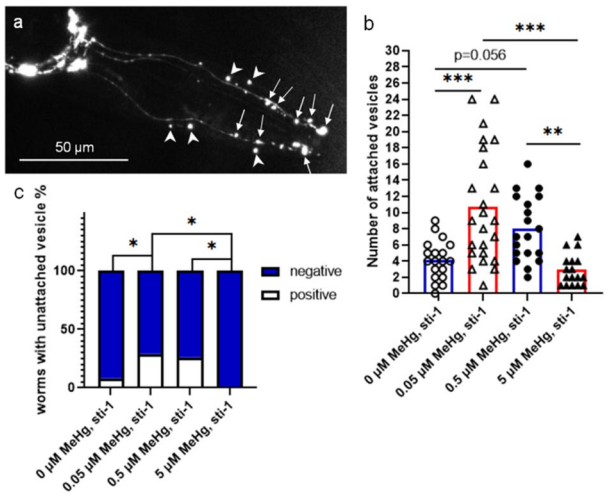

Fig. 3 Vesicular structures are increased following MeHg exposure in *sti-1* knockout strain. The VC2559*OH7193 strain was imaged at adult stage following MeHg treatment (0, 0.05, 0.5, and 5 µM) in NGM medium for 7 days. **a** Shows an adult stage with multiple attached vesicles (arrow) and unattached vesicles (arrow head) in CEP dendrites. **b** Number of attached vesicles in CEP dendrites in worms treated with MeHg. Analysis was made with one-way ANOVA and Tukey's multiple comparisons test. ***$P < 0.001$, and **$P < 0.01$. **c** Percentage of worms with positive unattached vesicle in CEP dendrites following MeHg treatment (the unattached vesicles were absent in nearly two thirds of the worms during the observation, so the data was categorized based on the presence of unattached vesicles). Analysis was made with Chi-square test. *$P < 0.05$

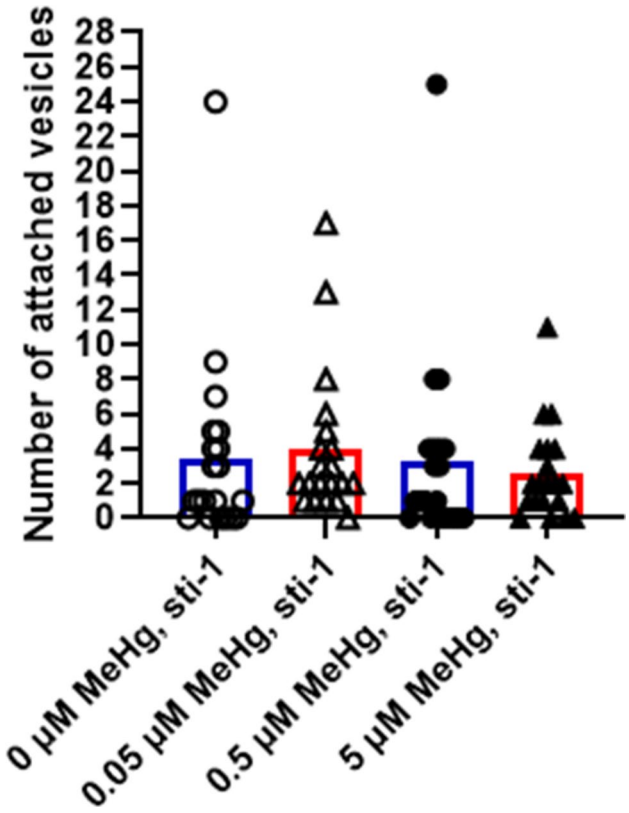

Fig. 4 Number of attached vesicles is not changed post MeHg treatment in the *sti-1* knockout strain. The L1 stage VC2559*OH7193 strain was treated with MeHg for 5 days in NGM medium, followed by 2 days on NGM plates. Number of CEP attached vesicles in adult stage worms was counted. Analysis of data: one-way ANOVA

the OH7193 strain to generate OH7193*TU3311 strain. The OH7193*TU3311 strain was fed with RNAi bacteria before MeHg treatment. We found that RNAi knockdown of *sti-1* in the OH7193*TU3311 strain failed to alter the number of attached vesicles, and a 24-h treatment with 5 µM MeHg had no significant effect in the RNAi control and *sti-1* knockdown worms (Fig. 7).

Discussion

The present study established that *C. elegans* CEP neuronal morphology has a significant transition from L3 to adult stage, with a prominent presence of vesicular structure in CEP dendrites in adult stage worms. MeHg exposure alters the number of attached vesicles and unattached vesicles in CEP neurons of the *sti-1* strain. The morphological changes induced by MeHg in the *sti-1* strain are dose- dependent. Moreover, there is an interactive effect of MeHg and *sti-1* on the number of attached vesicles. The induction of vesicular structures by MeHg may protect the cell from neurotoxic effects initially, but eventually cause the spread of toxic inclusions in the vesicles within neuronal tissues, leading to a vicious cycle to propagate the neurotoxic effects.

It has been shown that neurons of adult stage *C. elegans* are capable of generating large extracellular vesicles (approximately 4 µm in diameter) by budding-off from the plasma membrane of neuronal soma [22]. The inclusions of the vesicles contain protein aggregates including the fluorescent protein mCherry and damaged mitochondria, which are degraded remotely. Intriguingly, inhibition of protein quality control pathways, such as chaperones, autophagy or proteasome, significantly increases the number of vesicle, corroborating that formation of vesicle is a response to an overload of protein misfolding or decline in protein quality control [22]. The novel results from the current study show that there is a developmentally-dependent regulation of attached vesicles in CEP dendrites: the vesicular structure is adult-stage dependent (Fig. 1), and it likely maintains proteostasis by removing spatially organized mCherry via release of extracellular vesicles (Figs. 3 and 4, and discussions below) [3, 24]. It has been previously illustrated that there are checkpoints at the late larvae stages (L3 and L4) to coordinate the development and stress stimuli [25]. The development-dependent phenotypes observed in the current

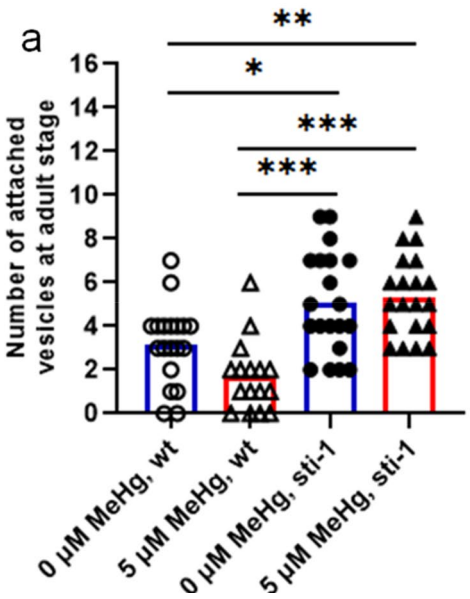

b

	SS	DF	F	P value
sti-1	143.418	1	38.649	<0.001
MeHg	6.367	1	1.716	0.194
interaction	14.569	1	3.926	0.050

Fig. 5 The CEP phenotypes in *sti-1* knockout strain are modulated by MeHg. The L1 stage OH7193 and VC2559*OH7193 strain were treated with MeHg for 5 days in NGM medium, followed by 2 days on NGM plates. **a** Number of CEP attached vesicles in adult stage worms. The worms treated with MeHg for 5 days were placed in OP50-seeded NGM plates for 2 days before evaluation. *P < 0.05, **P < 0.01, and ***P < 0.001. **b** Two-way ANOVA analysis of strain and MeHg effects. SS, sum of squares for genotype, MeHg treatment and the interaction term of genotype and MeHg; DF, degree of freedom

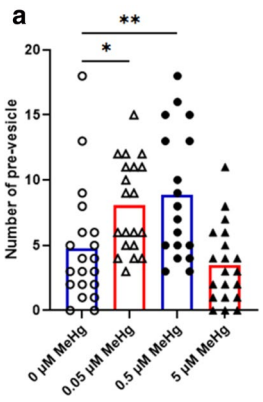

b

	MeHg, μM			
	0	0.05	0.5	5
vesicle numbers (positive worms/ total worms)	0 (0/20)	1 (1/20)	1 (1/18)	0 (0/20)

Fig. 6 The number of attached vesicles is increased with MeHg in adult stage worms of *sti-1* knockout strain. The adult stage VC2559*OH7193 worms were treated with MeHg (0, 0.05, 0.5, 5 μM) for 24 h in NGM medium before evaluation of CEP dendrites. **a** Numbers of CEP attached vesicles in worms treated with MeHg. **b** Numbers of CEP unattached vesicles in worms treated with MeHg. Analysis was made with one-way ANOVA and Tukey's multiple comparisons test. *P < 0.05, **P < 0.01

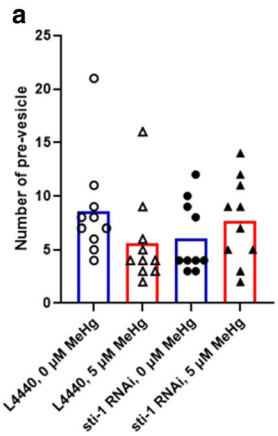

b

	SS	DF	F	P value
RNAi *sti-1*	0.400	1	0.024	0.878
MeHg	4.900	1	0.293	0.592
Interaction	52.900	1	3.165	0.084

Fig. 7 Knockdown *sti-1* does not alter the numbers of attached vesicles. The OH7193 strain was crossed with the TU3311 strain to generate a hypersensitive neuronal RNAi strain with DAergic expression of mCherry (OH7193*TU3311). The adult stage F1 generation of the OH7193*TU3311 strain fed with RNAi bacteria were treated with MeHg for 24 h. **a** Numbers of the CEP attached vesicles in the OH7193*TU3311 strain treated with MeHg. **b** Two-ANOVA analysis of the effect of RNAi *sti-1* and MeHg on the numbers of attached vesicles

study are possibly controlled by a neuronal program that is tightly coupled with cycles of development [26–29].

In the *sti-1* knockout strain, relatively low concentrations of MeHg (0.05 μM) increased the percentage of worms with compromised mCherry fluorescence of CEP neurons (Fig. 2b, c); however, a higher dose (5 μM) had no effect (Fig. 2d). These data are in agreement with the data from Fig. 3 showing that the number of attached vesicles and unattached vesicle was altered after upon 0.05 μM MeHg treatment, but not 5 μM MeHg. The genesis of extracellular vesicle is controlled by intracellular Ca^{2+} (Taylor et al., 2020), and MeHg can induce influx of Ca^{2+} and exert dose,

time-dependent effects on Ca^{2+} entry [30]. Thus, we postulated that, in the *sti-1* knockout background, low levels of MeHg (0.05–0.5 µM), could induce the formation of vesicle through a stimulatory effect on Ca^{2+} entry, leading to the loss of mCherry fluorescence. Perhaps, 5 µM MeHg caused an acute fast initial effect that would be attained gradually by 0.05 and 0.5 µM MeHg, but subsequently 5 µM MeHg dysregulated completely the Ca^{2+} signaling, depleting the Ca^{2+} stores and exhausting the pool of vesicles to be released. In our model, the effects of MeHg at 5 µM on the formation of attached vesicles could be masked at the late phase when the Ca^{2+} signaling was disrupted, whereas the effects could be observed at the relatively lower doses (0.05–0.5 µM) (Fig. 4). Corroboratively, it was proposed that the lower level of MeHg (0.5 µM) needs a longer time to reach the cellular targets compared to the dose at 5 µM [31]. In rat cerebellar granule cells, low levels of MeHg (0.2–0.5 µM) could induce Ca^{2+} influx, and the time to onset of Ca^{2+} influx was significantly longer for 0.5 µM MeHg (> 20 min) than 5 µM MeHg (~ 5 min) [31]. Because of the highly electrophilic activity of MeHg and its abundant cellular targets, the toxicity of or cellular response to MeHg is a combined output of multiple mechanisms [30, 32]. In addition to calcium signaling, energy insufficiency due to collapse in the mitochondria membrane potential might also have involved in the dose-dependent effects of MeHg on attached vesicles. In previous studies, we showed that MeHg (0–10 µM) dose-dependently reduced the mitochondria membrane potential in primary astrocyte cultures [33, 34].

The loss of mCherry fluorescence in the *sti-1* knockout worms post 12 h of MeHg treatment (5 µM) suggests that the loss of membrane components marked with mCherry fluorescence could be utilized as a clearance pathway to remove damaged organelles and proteins through vesicle formation and release, as reported earlier [22]. In a forward genetic screening for genes modulating the toxicity of 6-hydroxydopamine (6-OHDA), it was demonstrated that worms with loss-of-function mutation in *tsp-17* were hypersensitive to changes in DAergic morphology (loss of fluorescence) induced by 6-hydroxydopamine (OHDA) [21]. *Tsp-17* encodes a member of membrane proteins of the tetraspanin family. It has been shown that tetraspanin-4 (TSPAN4), also a member of the tetraspanin family, is a marker for the extracellular vesicles [35]. Combined with the data from these studies [21, 22, 35], our data suggest a model for the interpretation of the loss of mCherry fluorescence in CEP neurons (Fig. 2b, c): toxicant-induced vesicle formation dissipates the concentration of mCherry in the CEP dendrites to the level below the detection limit, and the vesicles from CEP neuronal soma causes the shrinkage shape of the soma (Fig. 2b) or complete loss of the signal (Fig. 2c); a period (12 h) post-treatment, worms that dosed with a higher concentration of MeHg were able to initiate the vesicle formation process, exhibiting a similar phenotype as worms evaluated shortly after treatment with 0.05 or 0.5 µM MeHg. We have previously shown that treatment with MeHg at 5 µM induced the bright mCherry puncta in CEP dendrites [19], corroborating the findings herein that worms with 5 µM MeHg were unable to increase the number of attached vesicles and unattached vesicles after treatment (Fig. 3). From these data (Figs. 2 and 3), it can be inferred that *C. elegans* may invoke a clearing system (in this case by a route of neuronal vesicle formation and release) to cope with MeHg-induced neurotoxicity. In addition, the integrity of CEP dendrites as evidenced by mCherry fluorescence and morphology was normalized in *sti-1* knockout worms treated with 0.05 or 0.5 µM MeHg to the control level 12 h post treatment (Fig. 2e), reinforcing the idea that active genesis of vesicles is a cellular strategy to cope with toxic challenges arising from MeHg exposure. Further, the activity of the neuronal vesicle formation is a well-regulated process tailored to the threshold level of toxic challenges, which could be inhibited by high levels of MeHg (e.g. 5 µM) or induced by moderate (0.5 µM) to low (0.05 µM) levels of the toxicant.

Because the attached vesicles are developmentally regulated and increased by a low level of MeHg in the *sti-1* knockout strain, we compared the morphology of CEP neurons in the control and *sit-1* knockout strains, after a period when worms were at the adult stage (Fig. 4). Our findings established that the number of attached vesicles in adult stage worms with MeHg were not significantly different compared to the control (Fig. 4); however, in the adult-stage worms treated with MeHg for 24 h, low level MeHg treatment increased the number of attached vesicles and possibly the number of unattached vesicles (Fig. 6). These data suggest that the *sti-1* knockout strain is highly responsive to low levels of MeHg, and this is in line with previous reports that modulation of the chaperone pathway determines organismal as well as cellular sensitivity to the toxicity of MeHg [6, 12, 13].

As the extreme sensitivity of the *sti-1* knockout strain to MeHg in vesicle formation compared with the control strain, and vesicle formation is also a cellular strategy to maintain cellular proteostasis [3, 22], we investigated whether *sti-1* knockdown could recapitulate the phenotypes seen in the *sti-1* knockout strain. However, the experiments with neuronal specific RNAi demonstrated that knock-down of *sti-1* in the neuronal tissue failed to significantly alter the numbers of attached vesicles (Fig. 7), suggesting that the phenotype is specific to the *sti-1* knockout strain. Clearly, further investigations in this strain are warranted to determine the mechanisms of MeHg-induced vesicle formation. Results from experiments with the *sti-1* knockout strain and the OH7193 control (Figs. 2 and 5) corroborate the findings that *sti-1* is an important factor in CEP morphology. STI-1

has multiple roles in development as well as protein quality control [15, 18, 36], and our study provides novel evidence that the morphology of CEP neuron is modulated by STI-1. Though further biochemical studies are needed to dissect out the precise steps in which STI-1 is involved in the regulation of vesicular structures, the current study established a highly sensitive model (the *sti-1* knockout strain) for studying cellular and molecular effectors of MeHg-induced neurotoxicity. The model will aid further endeavors to investigate the molecular cascades for the initiation and maturation of CEP vesicles and its implication for neuronal protection strategies against MeHg-induced neurotoxicity. For example, as the low levels of MeHg (e.g., 0.05 μM), doses that were not able to alter significant CEP structural changes in the control strain (Fig. 2a) [19], were able to induce formation of attached vesicles and unattached vesicles in the *sti-1* knockout strain, it will be interesting to investigate genetic factors that modulate the vesicle formation in *sti-1* knockout background.

Taken together, in the present study we have characterized developmentally-controlled phenotypes including attached vesicles of CEP neurons in *C. elegans*. MeHg-induced discontinuation and loss of mCherry fluorescence in *sti-1* strain likely results from an influx of vesicle formation associated with MeHg exposure. MeHg treatment induced significant structural changes in CEP neurons of *sti-1* strain, and there was a significant interactive effect between *sti-1* and MeHg on the numbers of attached vesicles, highlighting the interaction of genetic and environmental factors in MeHg-induced neurotoxicity. Further investigations on the molecular entities involved in the regulation of CEP vesicles, particularly in the *sti-1* strain treated with MeHg, are warranted.

Acknowledgements This work was supported by the National Institutes of Health to MA (NIEHS R01ES007331 and R01ES010563). The authors thank the Analytical Imaging Facility (AIF) at Albert Einstein College of Medicine, which is sponsored by NCI cancer center support grant P30CA013330 and Shared Instrumentation Grant (SIG) 1S10OD023591-01. Some strains were provided by the CGC, which is funded by NIH Office of Research Infrastructure Programs (P40 OD010440).

Compliance with Ethical Standards

Conflict of interest The authors declare that they have no conflict of interest.

References

1. Hipp MS, Kasturi P, Hartl FU (2019) The proteostasis network and its decline in ageing. Nat Rev Mol Cell Biol 20:421–435
2. Ciechanover A, Kwon YT (2017) Protein quality control by molecular chaperones in neurodegeneration. Front Neurosci 11:185
3. Sontag EM, Samant RS, Frydman J (2017) Mechanisms and functions of spatial protein quality control. Annu Rev Biochem 86:97–122
4. Muchowski PJ, Wacker JL (2005) Modulation of neurodegeneration by molecular chaperones. Nat Rev Neurosci 6:11–22
5. Karagas MR, Choi AL, Oken E, Horvat M, Schoeny R, Kamai E, Cowell W, Grandjean P, Korrick S (2012) Evidence on the human health effects of low-level methylmercury exposure. Environ Health Perspect 120:799–806
6. Caito S, Zeng H, Aschner JL, Aschner M (2014) Methylmercury alters the activities of Hsp90 client proteins, prostaglandin E synthase/p23 (PGES/23) and nNOS. PLoS ONE 9:e98161
7. Aschner M, Aschner JL (1990) Mercury neurotoxicity: mechanisms of blood-brain barrier transport. Neurosci Biobehav Rev 14:169–176
8. Ajsuvakova OP, Tinkov AA, Aschner M, Rocha JBT, Michalke B, Skalnaya MG, Skalny AV, Butnariu M, Dadar M, Sarac I, Aaseth J, Bjørklund G (2020) Sulfhydryl groups as targets of mercury toxicity. Coord Chem Rev 417:213343
9. Nogara PA, Oliveira CS, Schmitz GL, Piquini PC, Farina M, Aschner M, Rocha JBT (2019) Methylmercury's chemistry: from the environment to the mammalian brain. Biochim Biophys Acta Gen Subj 1863:129284
10. Zou J, Guo Y, Guettouche T, Smith DF, Voellmy R (1998) Repression of heat shock transcription factor HSF1 activation by HSP90 (HSP90 complex) that forms a stress-sensitive complex with HSF1. Cell 94:471–480
11. Morimoto RI (1993) Cells in stress: transcriptional activation of heat shock genes. Science 259:1409–1410
12. Hashimoto-Torii K, Torii M, Fujimoto M, Nakai A, El Fatimy R, Mezger V, Ju MJ, Ishii S, Chao SH, Brennand KJ, Gage FH, Rakic P (2014) Roles of heat shock factor 1 in neuronal response to fetal environmental risks and its relevance to brain disorders. Neuron 82:560–572
13. Hwang GW, Ryoke K, Lee JY, Takahashi T, Naganuma A (2011) siRNA-mediated silencing of the gene for heat shock transcription factor 1 causes hypersensitivity to methylmercury in HEK293 cells. J Toxicol Sci 36:851–853
14. Chang HC, Nathan DF, Lindquist S (1997) In vivo analysis of the Hsp90 cochaperone Sti1 (p60). Mol Cell Biol 17:318–325
15. Odunuga OO, Longshaw VM, Blatch GL (2004) Hop: more than an Hsp70/Hsp90 adaptor protein. BioEssays 26:1058–1068
16. Wegele H, Wandinger SK, Schmid AB, Reinstein J, Buchner J (2006) Substrate transfer from the chaperone Hsp70 to Hsp90. J Mol Biol 356:802–811
17. Beraldo FH, Soares IN, Goncalves DF, Fan J, Thomas AA, Santos TG, Mohammad AH, Roffe M, Calder MD, Nikolova S, Hajj GN, Guimaraes AL, Massensini AR, Welch I, Betts DH, Gros R, Drangova M, Watson AJ, Bartha R, Prado VF, Martins VR, Prado MA (2013) Stress-inducible phosphoprotein 1 has unique cochaperone activity during development and regulates cellular response to ischemia via the prion protein. FASEB J 27:3594–3607
18. Song HO, Lee W, An K, Lee HS, Cho JH, Park ZY, Ahnn J (2009) *C. elegans* STI-1, the homolog of Sti1/Hop, is involved in aging and stress response. J Mol Biol 390:604–617
19. Ke T, Tsatsakis A, Santamaria A, Antunes Soare FA, Tinkov AA, Docea AO, Skalny A, Bowman AB, Aschner M (2020) Chronic exposure to methylmercury induces puncta formation in cephalic dopaminergic neurons in *Caenorhabditis elegans*. Neurotoxicology 77:105
20. Xu F, Kula-Eversole E, Iwanaszko M, Hutchison AL, Dinner A, Allada R (2019) Circadian clocks function in concert with heat shock organizing protein to modulate mutant huntingtin aggregation and toxicity. Cell Rep 27:59–70 (**e54**)

21. Masoudi N, Ibanez-Cruceyra P, Offenburger SL, Holmes A, Gartner A (2014) Tetraspanin (TSP-17) protects dopaminergic neurons against 6-OHDA-induced neurodegeneration in *C. elegans*. PLoS Genet 10:e1004767
22. Melentijevic I, Toth ML, Arnold ML, Guasp RJ, Harinath G, Nguyen KC, Taub D, Parker JA, Neri C, Gabel CV, Hall DH, Driscoll M (2017) C. elegans neurons jettison protein aggregates and mitochondria under neurotoxic stress. Nature 542:367–371
23. Ke T, Aschner MJN (2019) Bacteria affect *Caenorhabditis elegans* responses to MeHg toxicity. Neurotoxicology 75:129–135
24. Kaganovich D, Kopito R, Frydman J (2008) Misfolded proteins partition between two distinct quality control compartments. Nature 454:1088–1095
25. Schindler AJ, Baugh LR, Sherwood DR (2014) Identification of late larval stage developmental checkpoints in *Caenorhabditis elegans* regulated by insulin/IGF and steroid hormone signaling pathways. PLoS Genet 10:e1004426
26. Ren P, Lim CS, Johnsen R, Albert PS, Pilgrim D, Riddle DL (1996) Control of *C. elegans* larval development by neuronal expression of a TGF-beta homolog. Science 274:1389–1391
27. Bargmann CI, Horvitz HR (1991) Control of larval development by chemosensory neurons in *Caenorhabditis elegans*. Science 251:1243–1246
28. Kim K, Sato K, Shibuya M, Zeiger DM, Butcher RA, Ragains JR, Clardy J, Touhara K, Sengupta P (2009) Two chemoreceptors mediate developmental effects of dauer pheromone in *C. elegans*. Science 326:994–998
29. Schroeder NE, Androwski RJ, Rashid A, Lee H, Lee J, Barr MM (2013) Dauer-specific dendrite arborization in *C. elegans* is regulated by KPC-1/Furin. Curr Biol 23:1527–1535
30. Limke TL, Heidemann SR, Atchison WD (2004) Disruption of intraneuronal divalent cation regulation by methylmercury: are specific targets involved in altered neuronal development and cytotoxicity in methylmercury poisoning? Neurotoxicology 25:741–760
31. Marty MS, Atchison WD (1997) Pathways mediating Ca2+ entry in rat cerebellar granule cells following in vitro exposure to methyl mercury. Toxicol Appl Pharmacol 147:319–330
32. Farina M, Aschner M, Rocha JB (2011) Oxidative stress in MeHg-induced neurotoxicity. Toxicol Appl Pharmacol 256:405–417
33. Yin Z, Lee E, Ni M, Jiang H, Milatovic D, Rongzhu L, Farina M, Rocha JB, Aschner M (2011) Methylmercury-induced alterations in astrocyte functions are attenuated by ebselen. Neurotoxicology 32:291–299
34. Yin Z, Milatovic D, Aschner JL, Syversen T, Rocha JB, Souza DO, Sidoryk M, Albrecht J, Aschner M (2007) Methylmercury induces oxidative injury, alterations in permeability and glutamine transport in cultured astrocytes. Brain Res 1131:1–10
35. Ma L, Li Y, Peng J, Wu D, Zhao X, Cui Y, Chen L, Yan X, Du Y, Yu L (2015) Discovery of the migrasome, an organelle mediating release of cytoplasmic contents during cell migration. Cell Res 25:24–38
36. Baindur-Hudson S, Edkins AL, Blatch GL (2015) Hsp70/Hsp90 organising protein (hop): beyond interactions with chaperones and prion proteins. Subcell Biochem 78:69–90